Gondwana Research 47 (2017) 188–199

Contents lists available at ScienceDirect

Gondwana Research

journal homepage: www.elsevier.com/locate/gr

Geochronology, petrogenesis, and tectonic significance of the latest Devonian–early Carboniferous I-type granites in the Central Tianshan, NW China

Jiyuan Yin [a,b,c,*], Wen Chen [a], Wenjiao Xiao [b,d,e], Chao Yuan [f], Bin Zhang [a], Keda Cai [e], Xiaoping Long [g]

[a] Laboratory of Isotope Thermochronology, Institute of Geology, Chinese Academy of Geological Sciences, Beijing 100037, China
[b] State Key Laboratory of Lithospheric Evolution, Institute of Geology and Geophysics, Chinese Academy of Sciences, Beijing 100029, China
[c] State Key Laboratory of Ore Deposit Geochemistry, Institute of Geochemistry, Chinese Academy of Sciences, Guiyang 550002, China
[d] CAS Center for Excellence in Tibetan Plateau Earth Sciences, Beijing 100101, China
[e] Xinjiang Research Center for Mineral Resources, Xinjiang Institute of Ecology and Geography, Chinese Academy of Sciences, Urumqi 830011, China
[f] State Key Laboratory of Isotope Geochemistry, Guangzhou Institute of Geochemistry, Chinese Academy of Sciences, Guangzhou 510640, China
[g] Department of Geology, Northwest University, Xi'an 710069, China

ARTICLE INFO

Article history:
Received 29 November 2015
Received in revised form 6 February 2016
Accepted 23 February 2016
Available online 7 April 2016

Keywords:
I-type granite
Northern Tianshan Ocean
Slab roll-back
Central Tianshan

ABSTRACT

The latest Devonian–early Carboniferous granitic intrusions in the Central Tianshan block are composed mainly of monzogranites and granodiorites. Here we present the petrology, geochemistry, and in situ zircon U–Pb ages and Hf isotopes of these intrusions. Bulk geochemistry suggests that the monzogranites and granodiorites are high-K, calc-alkaline, I-type granites. LA-ICP-MS zircon dating shows that the monzogranites and granodiorites formed at ca. 362 Ma and ca. 354 Ma, respectively. They are characterized by relatively high initial $^{176}Hf/^{177}Hf$ ratios (0.282571–0.282764) and positive $\varepsilon_{Hf(t)}$ values (+2.1 to +7.2). We interpret them to have been derived from partial melting of the Mesoproterozoic metamorphic basement of the Tianshan block and a significant addition of juvenile material. Compared to the monzogranites, the granodiorites are characterized by higher Sr (373–599 ppm), low Y (12.5–20.5 ppm), and Yb (1.21–2.04 ppm) contents, with relatively higher Sr/Y (26–32) ratios, analogous to those of modern adakitic rocks. The differences in geochemical characteristics between the monzogranites and granodiorites may reflect differences in the P–T conditions experienced by the two lithologies during partial melting. We propose that the latest Devonian monzogranites were possibly generated by partial melting of the Tianshan Mesoproterozoic basement rock with an influx of juvenile material in an arc setting. However, the granodiorites were likely related to the slab roll-back of subducted north Tianshan Ocean during the early Carboniferous.

1. Introduction

The Central Asian Orogenic Belt (CAOB), which is one of the largest accretionary orogens on the Earth, lies between the Siberian cratons to the north, the European craton to the west, and the Tarim and north China cratons to the south (Jahn et al., 2000, 2004; Windley et al., 2007; Xiao et al., 2008, 2009a, 2009b; Han et al., 2011; Xiao et al., 2015; Fig. 1a). It is characterized by extensive Paleozoic lateral continental growth dominated by long-lasting accretion of multiple microcontinents, island arcs, oceanic plateaus, seamounts, ophiolites, and accretionary complexes (e.g., Windley et al., 2007; Xiao et al., 2008; Xiao and Santosh, 2014; Zhao et al., 2015).

The west–east trending Tianshan Orogen, situated in the southern part of the CAOB, extends for over 2500 km through Uzbekistan, Tajikistan, Kyrgyzstan, and Kazakhstan to Xinjiang in northwestern China (Fig. 1a, Şengör et al., 1993; Jahn et al., 2000; Xiao et al., 2004; Windley et al., 2007; Klemd et al., 2015; Scheltens et al., 2015). The Tianshan Orogen were formed by progressive Paleozoic subduction and accretion of several southern branches of the Paleo-Asian Ocean located between the Tarim Craton and the Junggar Block (e.g., Gao et al., 2009; Xiao et al., 2009a, 2009b; Wang et al., 2010, 2011; Zhu et al., 2011; Xiao et al., 2013; Xiao and Santosh, 2014). The Chinese part of the Tianshan Orogen represents the final collision zone between the Siberian and Tarim cratons. Therefore, it is an ideal area to uncover the accretionary and tectonic history of the CAOB (Xiao et al., 2008, 2009a, 2009b). The Chinese Tianshan Orogen is characterized by voluminous, multi-stage granitic intrusions and volcanic rocks (Tang et al., 2010; Dong et al., 2011; Long et al., 2011; Xu et al., 2013; Ma et al., 2014, 2015). However, the tectonic setting for the magmatism is still a matter of debate in the Chinese Tianshan Orogen. Some researchers have suggested an extensional setting for the late Paleozoic, such as an intra-continental rift or mantle plume during late Devonian–early

* Corresponding author at: Laboratory of Isotope Thermochronology, Institute of Geology, Chinese Academy of Geological Sciences, Beijing 100037, China.
E-mail address: yinjiyuan1983@163.com (J. Yin).

http://dx.doi.org/10.1016/j.gr.2016.02.012
1342-937X/

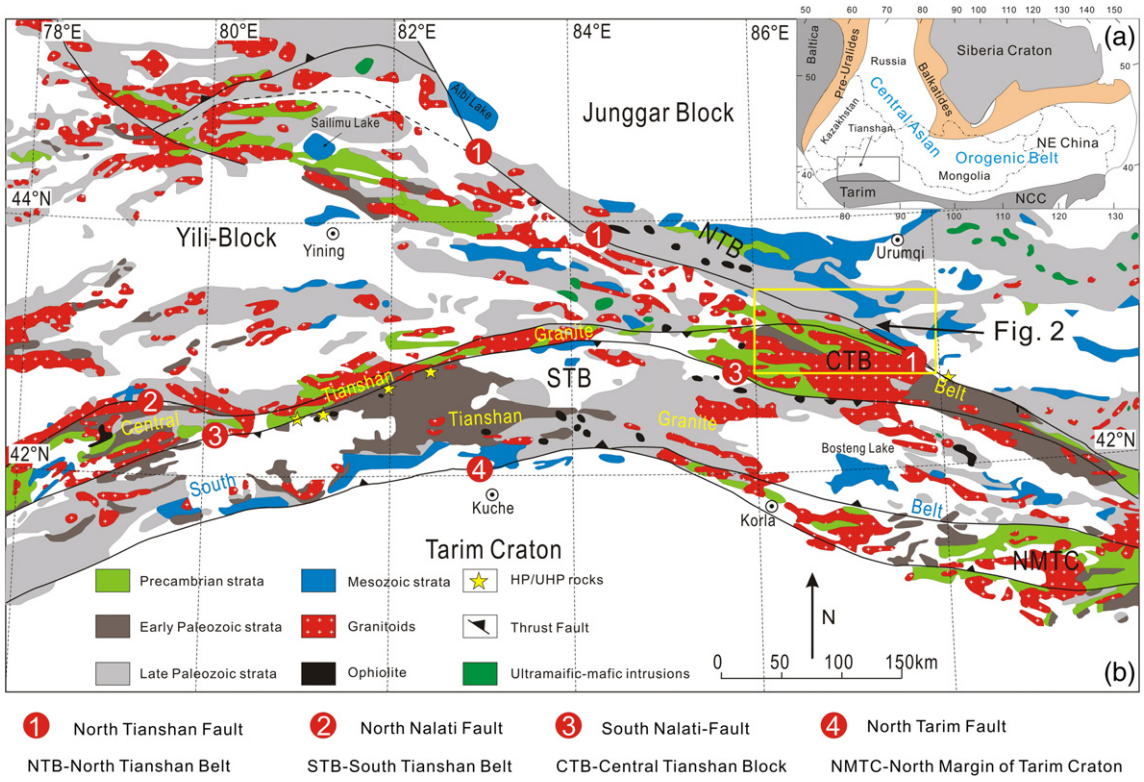

Fig. 1. (a) Simplified tectonic map of the Central Asian Orogenic Belt (Jahn et al., 2000). (b) Simplified geological map of the Chinese Tianshan (modified after Gao et al., 2009; Xiao et al., 2013).

Carboniferous (Xia et al., 2004a, 2004b, 2008), a post-collisional environment in early Carboniferous (Charvet et al., 2011) or in the late Carboniferous (Han et al., 2010, 2011; Long et al., 2011). Conversely, others have proposed that late Paleozoic magmatism was mainly related to subduction of the northern or southern Tianshan ocean (Tang et al., 2010, 2014; Li et al., 2015). Granitoids in the accretionary orogen can provide critical information on crustal growth and impose important constraints on the tectonic evolution of the CAOB. Previous studies, however, have mainly concentrated on early Paleozoic and late Carboniferous to Permian intrusions (Han et al., 2010; Dong et al., 2011; Lei et al., 2011; Tang et al., 2014; Ma et al., 2015) and Carboniferous volcanics (Zhu et al., 2005, 2009), with little attention to intrusions emplaced during the late Devonian to early Carboniferous. Recently, late Devonian to early Carboniferous magmatic plutons had been studied in the Central Tianshan (Ma et al., 2014). These are crucial for a comprehensive understanding of the Paleozoic subduction–accretion history of the Chinese Tianshan Orogen.

In this paper, we present new geochemical data, in situ zircon U–Pb ages, and zircon Hf isotopic data for representative granitic intrusions in Central Tianshan block in order to constrain the sources and petrogenesis of the intrusions and to resolve the geodynamic environment during their emplacement.

2. Geological setting and sampling

The Chinese Tianshan Orogen lies between the Junggar basin to the north and the Tarim basin to the south and has experienced a long, complex evolutionary history. From north to south, the Chinese Tianshan Orogen is tectonically subdivided into three main tectonic units: the North (NT), Central (CT), and South Tianshan (ST), which are separated by the Northern Tianshan suture (NTS) and the Southern Tianshan suture (STS) (Fig. 1b; Xiao et al., 2009a, 2009b, 2013; Klemd et al., 2015).

The NT represents a late Paleozoic continental magmatic arc-related to south-directed subduction of the northern Tianshan Ocean during the Paleozoic (Gao et al., 1998; Xiao et al., 2009a, 2009b). It is primarily composed of a series of early Devonian to late Permian sedimentary sequences and calc-alkaline volcanic and intrusive rocks, which are unconformably covered by Jurassic or Mesozoic clastic rocks (Xia et al., 2004a; Charvet et al., 2007). The ST is commonly considered to be a late Paleozoic accretionary complex formed in a back-arc basin (Kröner et al., 2013; Ma et al., 2014).

The CT can be divided into western and eastern region with different rock assemblages (Dong et al., 2011). The Western region, namely the Yili block, is dominated by a thick sequence of Proterozoic–Paleozoic sedimentary rocks and volcanic rocks (Che et al., 1994; Zhu et al., 2005; Wang et al., 2007; Zhu et al., 2009). The Eastern region is underlain by Proterozoic metamorphic basement rocks, mainly exposed in the Baluntai area in greenschist to amphibolite-facies (Che et al., 1994). In addition, there are Ordovician–Silurian meta-sedimentary rocks and Carboniferous–Permian sedimentary rocks in the Eastern region of the CT. Ages of the basement rocks are derived from a granitic gneiss dated to 948–926 Ma (Chen et al., 2009). Paleozoic (480–275 Ma) granitoids are widely distributed and intruded in the Eastern region of the CT (Yang et al., 2006; Shi et al., 2007; Gao et al., 2009; Dong et al., 2011; Gao et al., 2011; Zhu et al., 2011; Ma et al., 2014, 2015). Late Devonian to late Carboniferous island-arc-type volcanic and volcaniclastic rocks disconformably overlie late Silurian volcanics or the Proterozoic basement (Zhu et al., 2009; Tang et al., 2010, 2012).

We collected 23 samples of the Paleozoic monzogranites and granodiorites along the S301 road from Baluntai Town to Tuokexun County in the CT (Figs. 2, 3). Additional details, including sample locations and lithologies, are listed in Appendix 1.

The samples examined in this study do not show any petrographic evidence for metamorphism or alteration. The monzogranites consist of plagioclase (40+ vol.%), alkali feldspar (35 vol.%), quartz (20 vol.%), and biotite (<5 vol.%), with minor Fe–Ti oxides, apatite, and zircon (Fig. 4a, c). The granodiorites are composed of plagioclase (65 vol.%), alkali feldspar (10–15 vol.%), quartz 10–15 vol.%), and biotite (10–15 vol.%), with minor Fe–Ti oxides, apatite, zircon, and titanite (Fig. 4b, d).

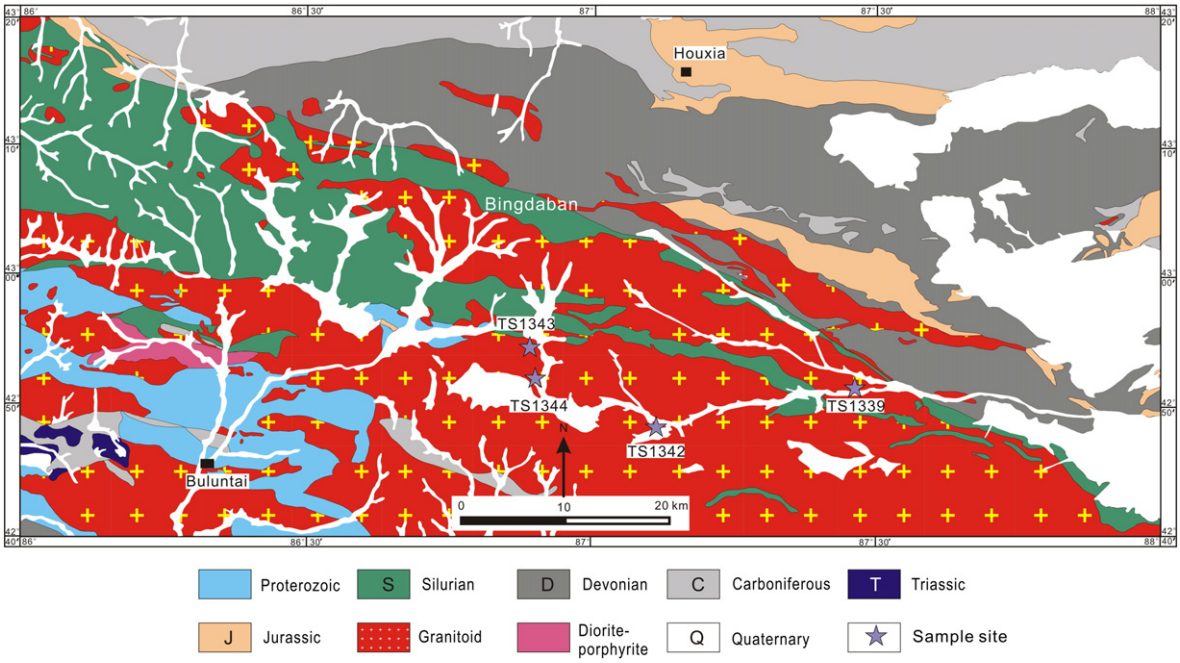

Fig. 2. Detailed geological map of Central Tianshan showing the sampling sites (after Yin et al., 2015a).

3. Methods

Major elements were analyzed by X–ray fluorescence spectrometry (XRF) on fused glass beads using a Rigaku 100e spectrometer at the State Key Laboratory of Isotope Geochemistry, Guangzhou Institute of geochemistry, Chinese Academy of Sciences (GIGCAS). Details of the procedures are described by Yuan et al. (2010) and Zhang et al. (2015).

Trace element concentrations, including rare earth element (REE) concentrations, were determined with a Perkin–Elmer ELAN–DRC–e inductively–coupled plasma mass spectrometer (ICP-MS) at the State Key Laboratory of Ore Deposit Geochemistry (SKLOG), Institute of

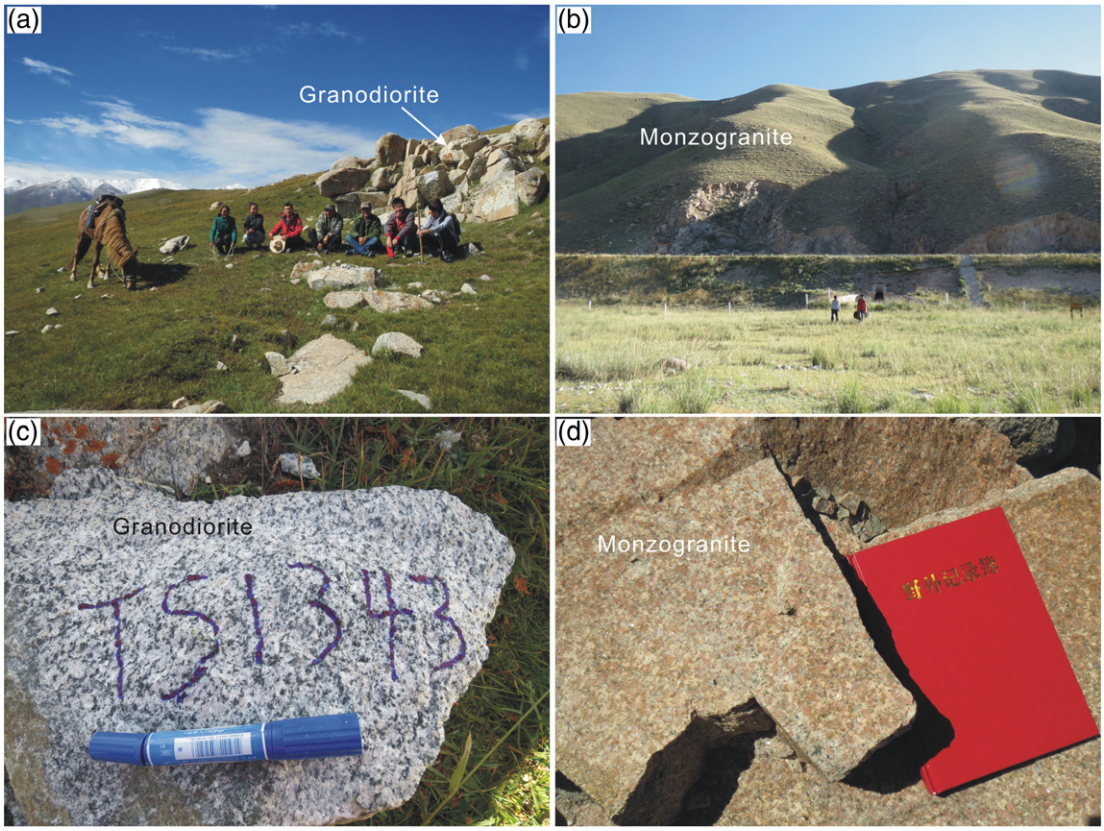

Fig. 3. Field photos of the Central Tianshan granitoid rocks.

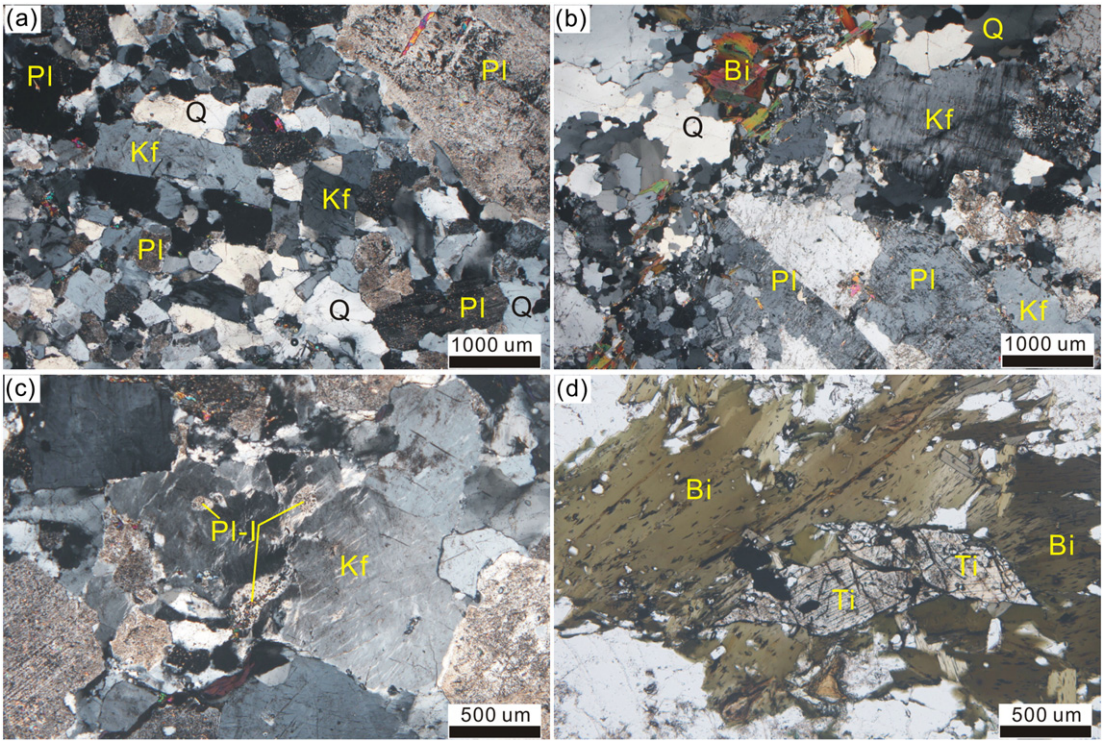

Fig. 4. Photomicrographs of Central Tianshan granitoid rocks. (a and c) Mineral compositions and textures of monzogranite; (b and d) mineral compositions and textures of granodiorite. Pl = plagioclase, Pl-I = plagioclase inclusion, Kf = Kfeldspar, Bi = biotite, Ti = titanite, Q = quartz.

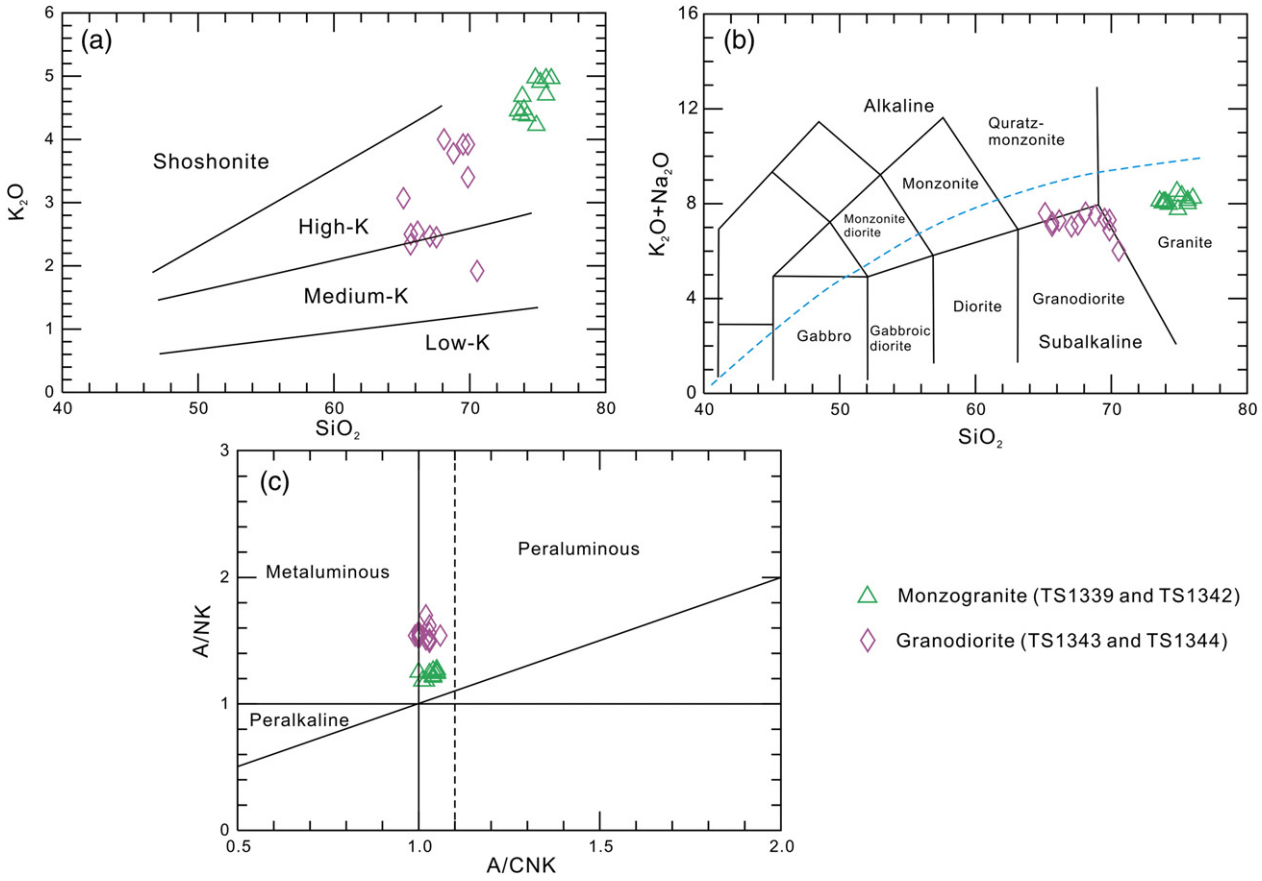

Fig. 5. Major and trace element discrimination diagrams for Central Tianshan granitoid rocks. (a) SiO_2 versus K_2O diagram (after Gill, 1981); (b) TAS classification diagram (after Middlemost, 1994), the alkaline and sub-alkaline division is after Irvine and Baragar (1971); (c) ANK versus ACNK diagram (Maniar and Piccoli, 1989).

Geochemistry, Chinese Academy of Sciences (IGCAS), following the procedures of Qi et al. (2000).

Zircon U–Pb isotopic compositions were analyzed with a VG PQ Excell ICP-MS equipped with a New Wave Research UV213 laser ablation system in the Department of Earth Sciences, the University of Hong Kong. The laser system delivers a beam of 213 nm UV light from a frequency quintupled Nd: YAG laser. Most analyses were carried out with a beam diameter of 30 μm, 6 Hz repetition rate. This gave a ^{238}U signal of 3×10^4 to 200×10^4 counts per second, depending on U contents. Typical ablation time was 30–60 s, resulting in pits 20–40 μm deep. Before measurement, samples were ablated for 10 s to eliminate common lead contamination on sample surfaces. Data acquisition started with a 15 s measurement of a gas blank during the laser warm-up time. The detailed analytical procedures are described by Geng et al. (2014).

In situ zircon Hf isotopic analyses were undertaken with a Neptune MC-ICP-MS at the Institute of Geology and Geophysics, Chinese Academy of Science. Detailed analytical procedures are described by Xie et al. (2008).

4. Results

4.1. Whole-rock geochemistry

4.1.1. The monzogranites

The monzogranites have SiO_2 concentrations ranging from 73.6 to 76.0 wt.% (Appendix 2). They show high K_2O (4.22–4.97 wt.%) and high $Na_2O + K_2O$ (7.75–8.51 wt.%), with high K_2O/Na_2O ratios (1.2–1.6) (Fig. 5a). In the TAS diagram (Fig. 5b), all samples are sub-alkaline and plot in the granite field. These rocks have low $Fe_2O_3^T$ (0.96–1.70 wt.%) and TiO_2 (0.12–0.22 wt.%), low MgO (0.15–0.43 wt.%) and low $Mg^{\#}$ (23–35). The monzogranites have low A/CNK ratios (1.00–1.05) and are slightly peraluminous (Fig. 5c).

These samples are moderately enriched in LREEs (e.g., $(La/Yb)_N$ = 5.1–10.8) and show relatively flat HREE patterns ($(Ga/Yb)_N$ = 0.72–3.1) with predominately negative Eu anomalies (Eu/Eu^* = 0.31–0.65) (Fig. 6a). These rocks are characterized by pronounced negative Ba, Nb, Ta, and Ti anomalies and positive Rb, Th, Pb spikes in a primitive mantle-normalized trace element variation diagram (Fig. 6b).

4.1.2. The granodiorites

The granodiorites, compared to the monzogranites, have lower SiO_2 (65.1–70.6 wt.%), K_2O (1.92–4.00 wt.%), and total alkalis ($Na_2O + K_2O$ = 6.02–7.63 wt.%) contents, but with relatively higher MgO (0.94–1.34 wt.%), $Mg^{\#}$ (38–43), Al_2O_3 (14.6–16.7 wt.%), $Fe_2O_3^T$ (2.69–4.34 wt.%), P_2O_5 (0.10–0.21 wt.%), and TiO_2 (0.37–0.66 wt.%). All samples are sub-alkaline and mostly plot in the granodiorite field (Appendix 2; Fig. 5b). They have low A/CNK ratios (0.99–1.06) and are slightly peraluminous (Fig. 5c).

The granodiorites are enriched in LREEs relative to HREEs with $(La/Yb)_N$ ratios of 17.2–28.5 and are characterized by weak negative Eu anomalies (Eu/Eu^* = 0.84–0.97) (Fig. 6c) except for one sample (TS1344-4). In a primitive mantle-normalized trace element variation diagram, the granodiorite samples show remarkable enrichment of LILEs (such as Ba, K, and Rb) relative to HFSEs and LREEs, with negative Nb–Ta–Ti anomalies (Fig. 6d), consistent with the geochemical characteristics of subduction-related magmas.

4.2. Zircon U–Pb age and Hf isotopic composition

4.2.1. The monzogranites

Thirteen zircons from monzogranite sample TS1342 were analyzed to constrain the crystallization age. The zircons are prismatic, transparent, and colorless with lengths ranging from 100 to 200 μm and widths from 60 to 100 μm (Fig. 7a). In CL images, they display well-preserved concentric oscillatory zoning with high Th/U ratios (0.58–1.32), which

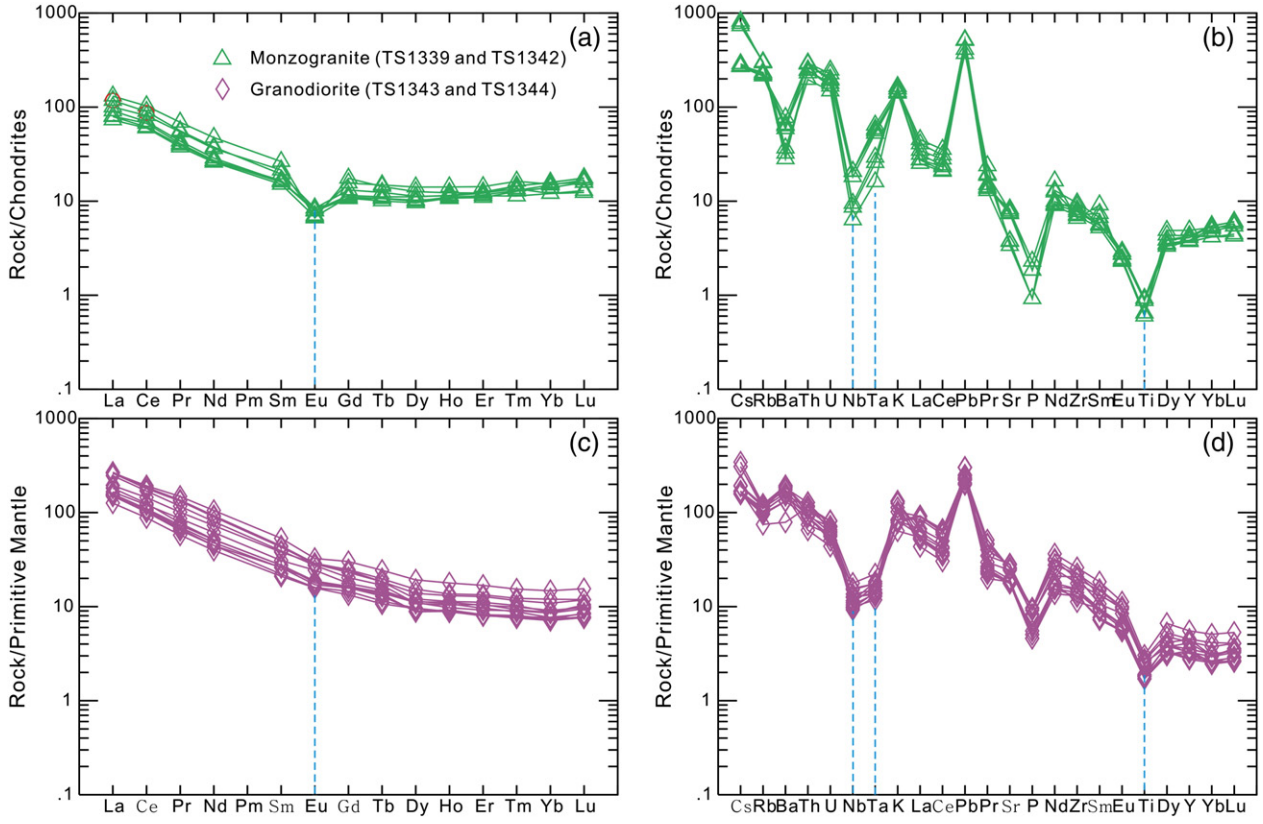

Fig. 6. Chondrite-normalized rare earth element patterns and primitive mantle-normalized trace element variation diagrams for Central Tianshan granitoid rocks. The chondrite and primitive mantle data are from Sun and McDonough (1989).

are indicative of a magmatic origin (Belousova et al., 2002). The zircons have $^{206}Pb/^{238}U$ dates varying from 364 to 358 Ma, with a mean of 362.2 ± 1.8 Ma, 1SD (MSWD = 0.47) (Appendix 3; Fig. 7a). We interpret this mean to as the crystallization age of sample TS1342. The zircon Lu–Hf analyses from sample TS1342 yielded relatively high initial $^{176}Hf/^{177}Hf$ ratios (0.282612–0.282739), corresponding to a variation of positive $\varepsilon_{Hf(t)}$ values (+2.1 to +6.1) with T_{2DM} ages ranging from 1.57 to 1.23 Ga (Fig. 8a, b).

4.2.2. The granodiorites

Zircon grains from both samples TS1343 and TS1344 are colorless in color, transparent to translucent, and occur as euhedral to prismatic crystals. The CL images show that all of the grains exhibit oscillatory zoning (Fig. 7b, c). Zircon grains from the granodiorites are 80–250 μm long, with 60–130 μm width. Their Th/U ratios are relatively high (0.61–1.30), consistent with a magmatic origin (Belousova et al., 2002).

Eleven zircons from sample TS1343 have similar apparent $^{206}Pb/^{238}U$ dates, ranging from 356 to 350 Ma (Appendix 3), and yield a weighted mean $^{206}Pb/^{238}U$ age of 353.9 ± 2.3 Ma, 1SD (MSWD = 0.13) (Fig. 7b). The Lu–Hf isotopic compositions of the same eleven zircons exhibit positive $\varepsilon_{Hf(t)}$ values (+2.3 to + 6.7) and relatively old T_{2DM} model ages (1.57–1.17 Ga) (Appendix 4; Fig. 8c, d).

Twelve zircon grains from sample TS1344 form a tight cluster on a concordia diagram (Fig. 7c) and have a weighted mean $^{206}Pb/^{238}U$ age of 353.6 ± 2.2 Ma, 1SD (MSWD = 0.28) (Fig. 7c), consistent with the age of sample TS1343 (Appendix 3). Twelve zircon grains from sample TS1344 were analyzed for Lu–Hf isotopic compositions (Appendix 4), which yielded similar $\varepsilon_{Hf(t)}$ values (+2.9 to +7.2) and T_{2DM} model ages (1.51–1.11 Ga) (Fig. 8c, d).

5. Discussion

5.1. Geochemical affinities

In general, granites can be divided into S-type, I-type, and A-type (Collins et al., 1982; Whalen et al., 1987). A-type granites typically contain high-temperature anhydrous phases such as pyroxene and fayalite, and late-crystallizing (interstitial) biotite and amphibole (e.g., King et al., 1997). The monzogranites and granodiorites that we studied contain biotite but lack pyroxene or fayalite, and the biotite is not a late-crystallizing phase (Fig. 4). The monzogranites and granodiorites all belong to the high-K series but have low Zr, Nb, and 10,000 × Ga/Al ratios, distinguishing them from A-type granites (Fig. 5a, c; Collins et al., 1982; Whalen et al., 1987). Further, all of the samples we studied fall within the field of I- and S-type granites (Fig. 9a). Chappell and White (1974) proposed that the boundary between S-type and I-type granites can be drawn at an A/CNK ratio of 1.1. The monzogranites and granodiorites all have low A/CNK ratio <1.1 (Fig. 5c) and exhibit a negative relationship between SiO_2 and P_2O_5, indicating a petrogenesis of I-type granites (Fig. 9b; Chappell and White, 1992; Chappell, 1999). These rocks have medium to high K_2O contents (Fig. 5a) and have a calc-alkaline affinity, consistent with the geochemical features of I-type granites. Additionally, S-type granites generally contain Al-rich minerals such as cordierite or muscovite. However, these minerals are not found in the samples we studied, further indicating that they are I-type granites rather than

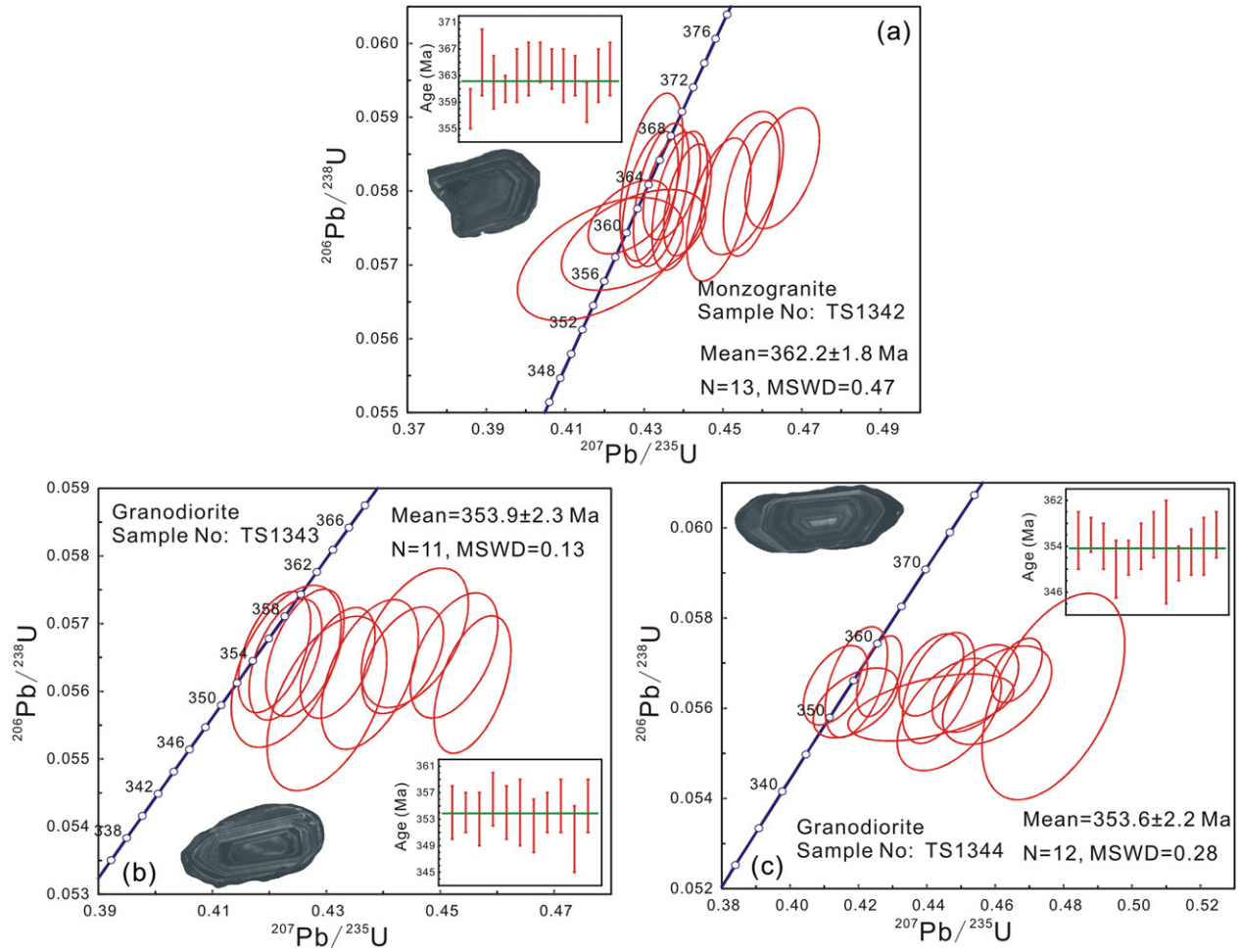

Fig. 7. Concordia diagrams for LA-ICP-MS zircon analyses of Central Tianshan granitoid rocks.

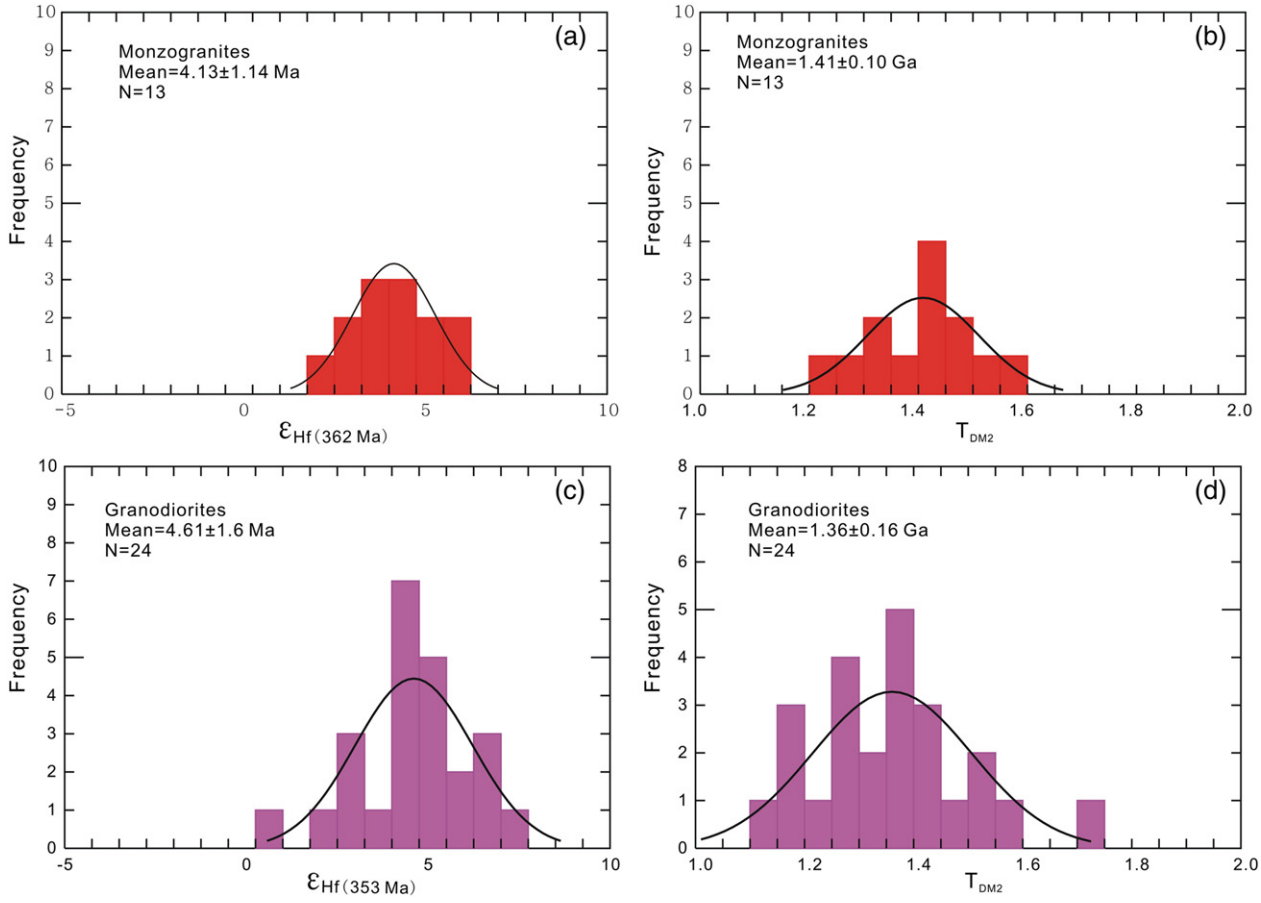

Fig. 8. (a) Histogram of $\varepsilon_{Hf(t)}$ for zircons with U–Pb age of ~353 Ma; (b) histogram of T_{DM2} for zircons with U–Pb ages of ~353 Ma; (c) histogram of $\varepsilon_{Hf(t)}$ for zircons with U–Pb ages of ~362 Ma; (d) histogram of T_{DM2} for zircons with U–Pb ages of ~362 Ma.

S-type granites. Finally, they are characterized by relative enrichments of LREEs and depletion of HFSEs (e.g., Nb, Ta, and Ti), relatively flat HREE patterns, and negative Eu anomalies, consistent with the geochemical characteristics of subduction-related magmas (Fig. 6b, d). In sum, our new evidences suggest that the monzogranites and granodiorites from Central Tianshan are I-type granites rather than A-type or S-type granites.

The granodiorites studied here are calc-alkaline (except for sample TS1344–2) and are characterized by high Sr (373–599 ppm), low Y (12.5–20.5 ppm), Yb (1.21–2.04 ppm), and relatively high Sr/Y (26–32) ratios. These characteristics are similar to those of adakite (Fig. 9c; Defant et al., 1992). Unlike granodiorites with adakitic characteristics, however, the monzogranites possess lower Sr content and Sr/Y ratios and do not fit the criteria of adakitic rocks (Fig. 9c; Defant et al., 1992).

5.2. Magma sources

The Central Tianshan I-type granites have low A/CNK ratios (<1.1, Fig. 5c) and exhibit a negative relationship between P_2O_5 and SiO_2, indicating that they were produced by partial melting of an igneous source (Chappell and White, 1992; Chappell, 1999). Three possible origins of granites have been proposed: (1) a crustal origin, (2) a mantle-derived origin, and (3) a mixed origin that involves both crustal and mantle-derived components (Barbarin, 1999). First, the Central Tianshan I-type granites have higher SiO_2 contents and relatively low MgO, $Mg^{\#}$, Cr, and Ni contents compared to magmas that could be derived from direct partial melting of the mantle, which usually have high $Mg^{\#}$ values and are no more silicic than andesitic compositions (Baker et al., 1995; Valley et al., 2005). Secondly, the physical and geochemical characteristics of the I-type granites are not consistent with mixing of mantle- and crust-derived melts. No mafic enclaves have been found in the pluton (Fig. 3c, d). Furthermore, the samples we studied have a narrow range of Hf isotopic compositions (Fig. 8a, c), which is atypical for magmas that incorporated both mantle and crustal components. In general, partial melting of the mafic or intermediate lower crust may account for the origin of I-type granites, which have been documented by field observations and related geochemical databases (Petford and Gallagher, 2001) as well as by experimental studies (Chappell, 1999). The similarity of Th/U ratios between the Central Tianshan I-type granites (average value of 6.89) and the lower crust (average value of 6, Rudnick and Gao, 2003) are consistent with a crustal origin. In addition, the monzogranites and granodiorites have similar zircon Hf isotopic compositions and $\varepsilon_{Hf(t)}$ values (Fig. 8a, c), indicating a common source or petrogenetic process. Their Mesoproterozoic T_{2DM} ages from Hf isotopes indicate that the Mesoproterozoic metamorphic basement of the Central Tianshan zone is one of the possible sources for the I-type granites. A number of Mesoproterozoic basements have been reported in the Central Tianshan and its surrounding areas. For example, there are 1.43–1.40 Ga granodiorites in East Tianshan (Hu et al., 2006), a 1.4 Ga granitic gneiss in Bingdaban of Central Tianshan (Chen et al., 2009), a 1.46–1.45 Ga Xingxingxia granitic gneiss in the east segment of the Central Tianshan (Shi et al., 2010), and an inherited zircon with age of ~1.4 Ga from the Xingxingxia granodiorite (Lei et al., 2011). Moreover, these zircons are also marked by positive $\varepsilon_{Hf(t)}$ values, implying that the juvenile material plays a key part in the formation of the monzogranites and granodiorites and mantle-derived material has been involved in the formation of the Paleozoic granitoids

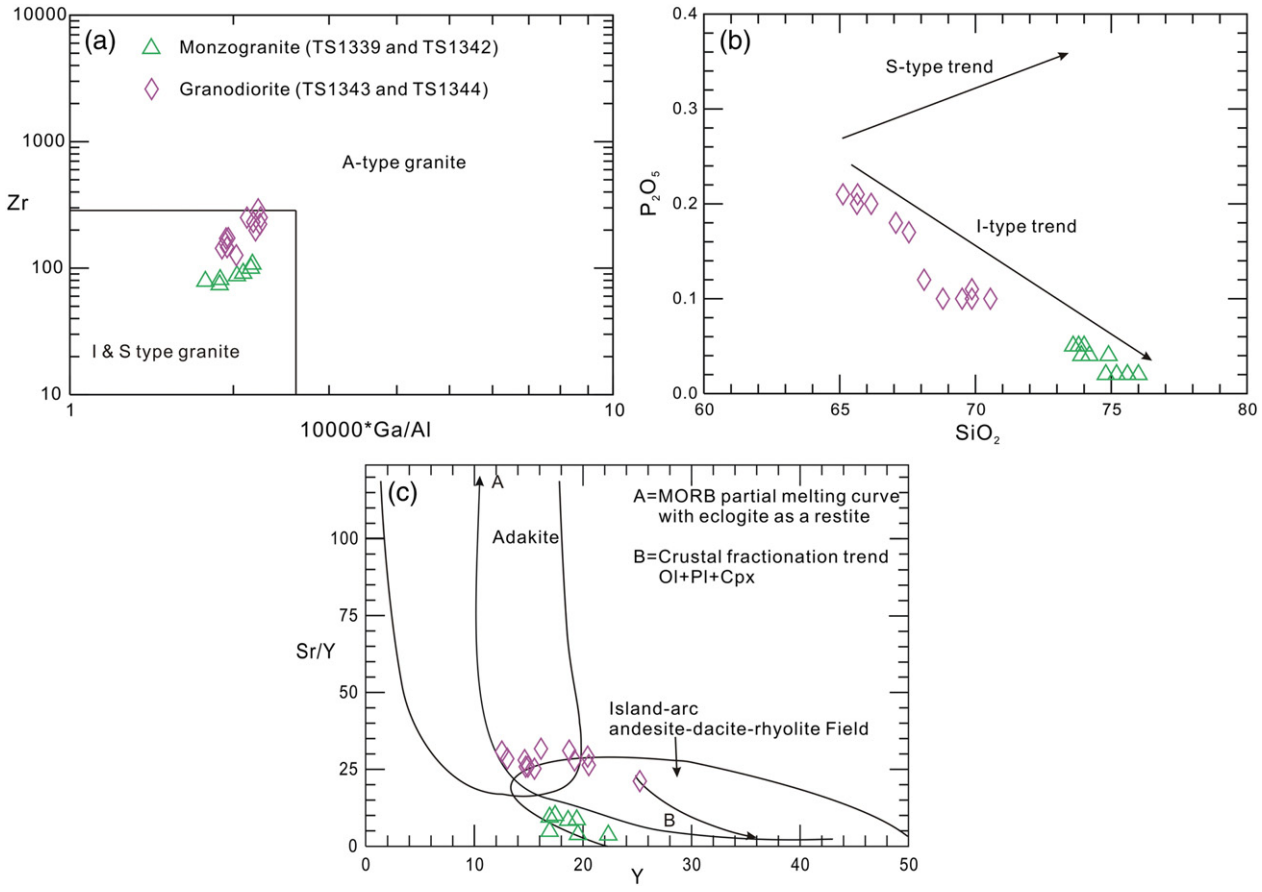

Fig. 9. (a) Zr vs. 10,000 Ga/Al discrimination diagrams (Whalen et al., 1987); (b) P_2O_5 vs. SiO_2 diagram, the trend of I- and S-type granites follows Chappell (1999); (c) Sr/Y versus Y (after Defant et al. (1992).

in the Central Tianshan. As a result, the magma sources of the monzogranites and granodiorites likely include both the Mesoproterozoic basement and juvenile material.

Although the granodiorites and monzogranites show similar zircon Hf isotopic compositions and $\varepsilon_{Hf(t)}$ values, they differ in some of their other geochemical features. For example, the granodiorites have high Sr (373–599 ppm) contents, low Y (12.5–20.5 ppm) and Yb (1.21–2.04 ppm) contents, and relatively high Sr/Y (26–32) ratios (Appendix 2), analogous to those of modern adakites. In contrast, the monzogranites exhibit lower Sr (71–174 ppm) contents and Sr/Y (3–10) ratios. Garnet and/or hornblende may have been major residual phases in the origin of the granodiorites. If garnet is a residual phase in the source, the resultant magmas will show strong HREE depletion, whereas relatively low Gd/Yb ratios and flat HREE patterns for the granodiorites would exclude garnet as a residual phase. The granodiorites show a progressive decrease in middle and heavy REEs with increasing atomic number (Fig. 6c), suggesting breakdown of amphibole in the source. This may have supplied enough water to induce partial melting of the middle to lower crust to generate granitic melt (Rapp and Watson, 1995; X.L. Huang et al., 2013). The breakdown of amphibole can progress through a variety of reactions under varying P–T conditions (Wyllie and Wolf, 1993; Wolf and Wyllie, 1994). In an anhydrous source in the middle to lower crust (<8 kbar), an extremely high temperatures (a high thermal gradient >35 °C/km) would be required for the breakdown of amphibole (X.L. Huang et al., 2013). However, the monzogranites do not show an obvious depletion of mid- to high REEs that indicate no breakdown of amphibole (Fig. 6a).

Therefore, we infer that the Central Tianshan granodiorites were formed by partial melting of Mesoproterozoic basement rocks with a significant addition of juvenile material at a relatively high thermal gradient (>35 °C/km). In contrast, the monzogranites were likely generated through partial melting of Mesoproterozoic basement rock with a significant addition of juvenile material at a relatively low thermal gradient (<35 °C/km). Thus, the granodiorites and monzogranites were likely formed from common source generated by partial melting under different P–T conditions.

5.3. Implications for tectonic evolution

The latest Devonian to early Carboniferous I-type granites are widespread in the Central Tianshan. They show relatively high-K, calc-alkaline characteristics (Fig. 5a), with LREE enrichments and negative anomalies of HFSEs, such as Nb, Ta, and Ti, and positive anomalies of LILEs (Fig. 6b, d). These features are consistent with arc magmas that are produced in subduction zones (Pearce et al., 1984). However, other researchers have previously proposed a variety of models to account for Carboniferous magmatism in the Central Tianshan. Xia et al. (2004a, 2008) suggested that Carboniferous magmatic rocks in the Tianshan Orogen represent a large igneous province related to a mantle plume. Another hypothesis is that the late Paleozoic granitoids were generated in a post-collisional setting (Dong et al., 2011; Xu et al., 2013). Finally, some researchers have posited that the granitoids were produced in an island-arc setting in the Tianshan Orogen during the Carboniferous (Tang et al., 2010, 2012; Yin et al., 2015a).

First, we note that zircon saturation temperature calculations for the I-type granites (749–814 °C) are significantly lower than those for Permian granites (800–1010 °C; data from Zhang et al., 2008, 2010), related to the Tarim mantle plume (Zhou et al., 2008). In addition, the Carboniferous volcanic rocks in the Tianshan are mainly calc-alkaline and intermediate-felsic in composition, with minor amounts of mafic

rocks. They also show enrichment in LILEs and depletion in HFSEs, akin to typical island arc-type volcanic rocks (Zhu et al., 2005). More importantly, plume-derived mafic rocks display more fractionated REE patterns, with pronounced peaks at Nb, Ta, and Ti, which are distinctive from those of Carboniferous volcanic rocks in the Tianshan. This suggests that the formation of the Central Tianshan I-type granites was not related to a Carboniferous mantle plume.

Second, it is unlikely that the Central Tianshan I-type granites were formed in a post-collisional setting. For example, they nearly plot in the volcanic arc granite (VAG) field in Nb–Y, Ta–Yb, Rb–(Yb + Ta) and Rb–(Y + Nb) discrimination diagrams (Fig. 10a-d, Pearce et al., 1984). Instead, we favor an arc-related tectonic setting based on the following geological evidence: (1) Late Carboniferous basaltic rocks and mafic dike–granitoid associations from the western Tianshan all show typical island arc-type geochemical characteristics, suggesting that their origins were related to oceanic subduction (Tang et al., 2012, 2014). (2) Carboniferous ophiolites have recently been identified in the area, e.g., the 344 ± 3 Ma Bayingou ophiolite in the western Tianshan (Xu et al., 2006). (3) The coexistence of sanukitoids, adakites, charnockites, alkali feldspar granites, and Cu–Au mineralization indicates a ridge subduction regime in the West Junggar during the Late Carboniferous–Early Permian (Geng et al., 2009; Yin et al., 2013, 2015b). These authors proposed that the collision between the Junggar Plate and the Yili Block likely occurred after the late Carboniferous. Thus, based on our newly obtained geochemical and Hf isotopic data and the previously published geological, geochronological and geochemical data, we suggest that the Central Tianshan I-type granites were formed in a subduction-related tectonic setting.

A number of ophiolite belts have been discovered on the north side of the Yili Block, including the Tangbale, Dalabuter, and Bayingou ophiolites, which formed between 531 and 325 Ma (Zhu et al., 1987; Zhang et al., 1993; Jian et al., 2005; Xu et al., 2006). While these ophiolites record the evolution of the northern Tianshan Ocean from at least the Early Cambrian to the Early Carboniferous, the exact closure time of the northern Tianshan Ocean remains debatable. Other researchers have suggested that the northern Tianshan Ocean closed in the Late Devonian (Xia et al., 2004a, 2004b), the Early Carboniferous (Han et al., 2010), the Late Carboniferous (Sun et al., 2008; Gao et al., 2009; Long et al., 2011), or the Permian–Triassic (Xiao et al., 2013, 2014; Xiao and Santosh, 2014; Li et al., 2015). Recently, a large variety of arc-type magmatic rocks from the Ordovician to Permian have been reported in the Chinese Tianshan.

The arc-related geochemical features of mafic and felsic rocks (463–448 Ma) in the northwestern Tianshan suggest that the southward subduction of oceanic crust in the northern Tianshan Ocean beneath the Yili Block initiated in the middle Ordovician (Z.Y. Huang et al., 2013). In addition, the latest early Carboniferous adakite-high Mg andesite-Nb-enriched arc basalt suites in the western Tianshan area likely formed from magmas produced by partial melting of a subducted oceanic slab (Wang et al., 2006). A paleomagnetic study shows that a large gap of several hundreds of kilometers was still present between the Junggar block and Yili–Central Tianshan terranes at ca. 320–304 Ma, and probably suggest that the northern Tianshan Ocean had not closed by the Late Carboniferous (Xiao et al., 2014; Yi et al., 2015). Finally, early Permian mylonitic granites in West Tianshan display enrichments of LILEs (e.g. Rb, Ba, and Th) and relative depletions of HFSEs (e.g. Nb, Ta, and Ti), indicating they are derived from an arc setting and that subduction of oceanic crust in the northern Tianshan Ocean probably continued until the early Permian (Li et al., 2015). The geochronology and geochemistry for the I-type granitoids in the present

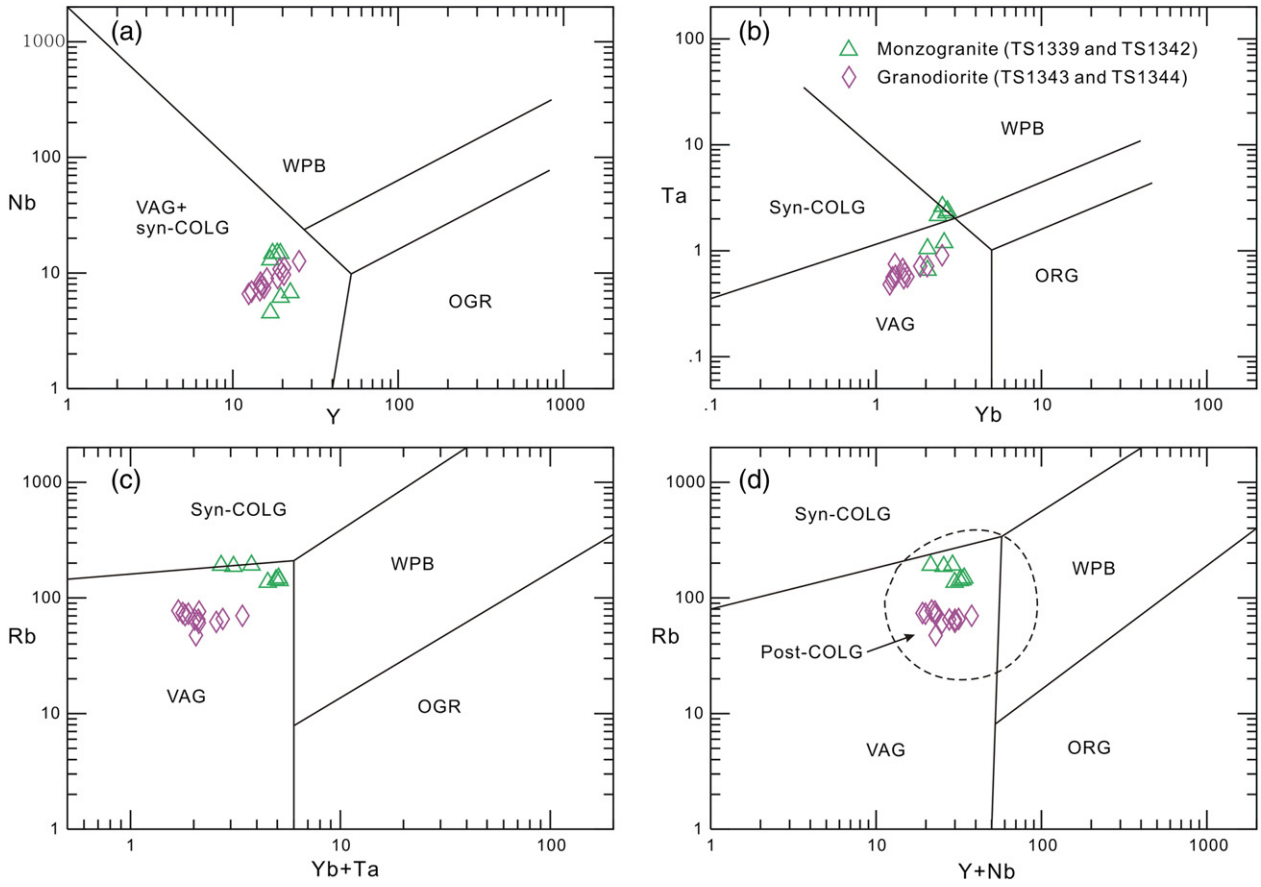

Fig. 10. Tectonic discriminating diagrams of Central Tianshan granitoid rocks. (a) Y versus Nb; (b) Yb versus Ta; (c) (Yb + Ta) versus Rb; (d) (Y + Nb) versus Rb (Pearce, 2008).

study, combined with previously published results, suggest that the Junggar block likely did not collide with the Yili–Central Tianshan terrane until the Permian.

The granodiorites studied here are analogous to those of modern adakites and were likely generated by the partial melting of the Tianshan Mesoproterozoic basement rock with remarkable involvement of juvenile component. We propose that the latest Devonian monzogranites were produced in an arc environment as oceanic crust in the northern Tianshan Ocean was subducted. Subsequently, the subducting slab began to roll-back, sinking quickly into the mantle and inducing upwelling of the asthenosphere to compensate for the loss in volume of the mantle wedge (Uyeda and Kanamori, 1979). The upwelling of hot asthenosphere triggered partial melting of Mesoproterozoic basement rocks and the important input of depleted mantle material generating granitic magmas (i.e. granodiorites) during the early Carboniferous (Jiang et al., 2006, 2011). Finally, partial melting of depleted mantle material produced the basaltic magma in the west Tianshan in the early Carboniferous (Zhu et al., 2009; An et al., 2013).

6. Conclusions

Two type granitoids in the Central Tianshan, namely, monzogranites and granodiorites, have been investigated in order to provide some important constraints on their sources and petrogenesis and to resolve the geodynamic environment during their emplacement.

(1) LA-ICP-MS zircon dating indicates that the monzogranites and granodiorites formed at ca. 362 Ma and ca. 354 Ma, respectively.
(2) The two type granitoids show similar zircon Hf isotopic compositions and $\varepsilon_{Hf(t)}$ values that suggest a common source. They were likely derived from partial melting of the Mesoproterozoic metamorphic basement of the Tianshan block and significant input of juvenile material.
(3) The differences in geochemical characteristics between the monzogranites and granodiorites are likely formed by partial melting under different P–T conditions.
(4) The latest Devonian monzogranites were probably generated by partial melting of the Tianshan Mesoproterozoic basement rock and the remarkable involvement of juvenile material due to normal southward subduction of oceanic crust in the northern Tianshan Ocean. Subsequently, the subduction angle changed from normal to steep and induced upwelling of hot asthenosphere. This caused partial melting of Mesoproterozoic basement rock and the input of depleted mantle material under comparatively higher temperature conditions, generating the parent magmas that intruded to form the Central Tianshan granodiorites in the early Carboniferous.

Supplementary data to this article can be found online at http://dx.doi.org/10.1016/j.gr.2016.02.012.

Acknowledgments

This study was supported by the Major Basic Research Project of the Ministry of Science and Technology of China (grant no: 2014CB448000), National Science Foundation of China (grant nos. 41390441, 41473053, 41273012, 41230207, 41390441, 41203026, 41573045), a grant of Chinese Ministry of Land and Resources (grant no. 201211074–05), and an open fund from the State Key Laboratory of Ore Deposit Geochemistry, Institute of Geochemistry, Chinese Academy of Sciences (grant no. 201401), China Scholarship Council (file no. 201409110006), China Postdoctoral Science Foundation (grant nos. 2014M560113, 2015 T80134), the China Geological Survey (grant no. 12120113015600). We are grateful to Professor M. Santosh and two anonymous reviewers for their critically constructive reviews, which allowed us to improve the present discussion greatly. We also express our appreciation to Dr. Gongjian Tang, Hongyan Geng, and Cameron M. Mercer for their critical reading and polishing of the manuscript. We also thank Dr. Yueheng Yang, Li Yang, Hongyan Geng, Jean Wong, and Jing Hu for laboratory assistance. This is a contribution to IGCP592.

References

An, F., Zhu, Y., Wei, S., Lai, S., 2013. An Early Devonian to Early Carboniferous volcanic arc in North Tianshan, NW China: geochronological and geochemical evidence from volcanic rocks. Journal of Asian Earth Sciences 78, 100–113.
Baker, M.B., Hirschmann, M.M., Ghiorso, M.S., Stolper, E.M., 1995. Compositions of near solidus peridotite melts from experiments and thermodynamic calculations. Nature 375, 308–311.
Barbarin, B., 1999. A review of the relationships between granitoid types, their origins and their geodynamic environments. Lithos 46, 605–626.
Belousova, E.A., Griffin, W.L., Suzanne, Y.O.R., Fisher, N.I., 2002. Igneous zircon: trace element composition as an indicator of source rock type. Contributions to Mineralogy and Petrology 143 (5), 602–622.
Chappell, B.W., 1999. Aluminium saturation in I- and S-type granites and the characterization of fractionated haplogranites. Lithos 46, 535–551.
Chappell, B.W., White, A.J.R., 1974. Two contrasting granite types. Pacific Geology 8, 173–174.
Chappell, B.W., White, A.J.R., 1992. I- and S-type granites in the Lachlan Fold Belt. Transactions of the Royal Society of Edinburgh: Earth Sciences 83, 1–26.
Charvet, J., Shu, L.S., Laurent-Charvet, S., 2007. Paleozoic structural and geodynamic evolution of eastern Tianshan (NW China): welding of the Tarim and Junggar plates. Episodes 30, 162–186.
Charvet, J., Shu, L., Laurent-Charvet, S., Wang, B., Faure, M., Cluzel, D., Chen, Y., De Jong, K., 2011. Palaeozoic tectonic evolution of the Tianshan belt, NW China. Science China Earth Sciences 54, 166–184.
Che, Z.C., Liu, H.F., Liu, L., 1994. Formation and Evolution of the Middle Tianshan Orogenic Belt. Geological Publishing House, Beijing, pp. 1–135.
Chen, X.Y., Wang, Y.J., Sun, L.H., Fan, W.M., 2009. Zircon SHRIMP U–Pb dating of the granitic gneisses from Bingdaban and Laerdundaban (Tianshan orogen) and their geological significances. Geochimica 38, 424–431 (in Chinese with English abstract).
Collins, W.J., Beams, S.D., White, A.J.R., Chappell, B.W., 1982. Nature and origin of A-type granites with particular reference to Southeastern Australia. Contributions to Mineralogy and Petrology 80, 189–200.
Defant, M.J., Jackson, T.E., Drummond, M.S., De Boer, J.Z., Bellon, H., Feigenson, M.D., Maury, R.C., Stewart, R.H., 1992. The geochemistry of young volcanism throughout Western Panama and southeastern Costa Rica: an overview. Journal of the Geological Society, London 149, 569–579.
Dong, Y.P., Zhang, G.W., Neubauer, F., Liu, X.M., Hauzenberger, C., Zhou, D.W., Li, W., 2011. Syn– and post–collisional granitoids in the Central Tianshan orogen: geochemistry, geochronology and implications for tectonic evolution. Gondwana Research 20, 568–581.
Gao, J., Li, M., Xiao, X., Tang, Y., He, G., 1998. Paleozoic tectonic evolution of the Tianshan orogen, Northwestern China. Tectonophysics 287, 213–231.
Gao, J., Long, L.L., Klemd, R., Qian, Q., Liu, D.Y., Xiong, X.M., Su, W., W.L., Wang, Y.T., Yang, F.Q., 2009. Tectonic evolution of the Southern Tianshan orogen, NW China: geochemical and age constraints of granitoid rocks. International Journal of Earth Sciences 98, 1221–1238.
Gao, J., Klemd, R., Qian, Q., Zhang, X., Li, J.L., Jiang, T., Yang, Y.Q., 2011. The collision between the Yili and Tarim blocks of the Southwestern Altaids: geochemical and age constraints of a leucogranite dike crosscutting the HP–LT metamorphic belt in the Chinese Tianshan orogen. Tectonophysics 499, 118–131.
Geng, H.Y., Sun, M., Yuan, C., Xiao, W.J., Zhao, G.C., Zhang, L.F., Wong, K., Wu, F.Y., 2009. Geochemical, Sr–Nd and zircon U–Pb–Hf isotopic studies of late carboniferous magmatism in the west Junggar, Xinjiang: implications for ridge subduction? Chemical Geology 266, 364–389.
Geng, H.Y., Brandl, G., Sun, M., Wong, J., Kröner, A., 2014. Zircon ages defining deposition of the Palaeoproterozoic Soutpansberg Group and further evidence for Eoarchaean crust in South Africa. Precambrian Research 249, 247–262.
Gill, T.B., 1981. Orogenic Andesite and Plate Tectonics. Springer–Verlag, Berlin, p. 390.
Han, B.F., Guo, Z.J., Zhang, Z.C., Zheng, L., Chen, J.F., Song, B., 2010. Age, geochemistry, and tectonic implications of a Late Paleozoic stitching pluton in the North Tian Shan suture zone, Western China. Geological Society of America Bulletin 122, 627–640.
Han, B.F., He, G.Q., Wang, X.C., Guo, Z.J., 2011. Late carboniferous collision between the Tarim and Kazakhstan–Yili terranes in the western segment of the South Tian Shan Orogen, Central Asia, and implications for the North Xinjiang, Western China. Earth Science Reviews 109, 74–93.
Hu, A.Q., Wei, G.J., Deng, W.F., Zhang, J.B., Chen, L.L., 2006. 1.4 Ga SHRIMP U–Pb age for zircons of granodiorite and its geological significance from the eastern segment of the Tianshan Mountains, Xinjiang, China. Geochimica 35, 333–345 (in Chinese with English abstract).
Huang, X.L., Yu, Y., Li, J., Tong, L.X., Chen, J.L., 2013a. Geochronology and petrogenesis of the early Paleozoic I-type granite in the Taishan area, South China: middle–lower crustal melting during orogenic collapse. Lithos 177, 268–284.
Huang, Z.Y., Long, X.P., Kröner, A., Yuan, C., Wang, Q., Sun, M., Zhao, G.C., Wang, Y.J., 2013b. Geochemistry, zircon U–Pb ages and Lu–Hf isotopes of early Paleozoic plutons in the northwestern Chinese Tianshan: petrogenesis and geological implications. Lithos 182-183, 48–66.

Irvine, T.N., Baragar, W.R.A., 1971. A guide to the chemical classification of the common volcanic rocks. Canadian Journal of Earth Sciences 8, 523–548.
Jahn, B.M., Wu, F., Chen, B., 2000. Massive granitoid generation in Central Asian: Nd isotope evidence and implication for continental growth in the Phanerozoic. Episodes 23, 82–92.
Jahn, B.M., Windley, B., Natal'in, B., Dobretsov, N., 2004. Phanerozoic continental growth in Central Asia. Journal of Asian Earth Sciences 23, 599–603.
Jian, P., Liu, D.Y., Shi, Y.R., Zhang, F.Q., 2005. SHRIMP dating of SSZ ophiolites from northern Xinjiang Province, China: implications for generation of oceanic crust in the Central Asian Orogenic Belt. In: Sklyarov, E.V. (Ed.), Structural and Tectonic Correlation across the Central Asia Orogenic Collage: North-Eastern Segment; Guide-Book and Abstract Volume of the Siberian Workshop IGCP-480. Institute of the Earth Crust, Siberian Branch of Russian Academy of Sciences, Irkutsk, pp. 1–246.
Jiang, Y.H., Jiang, S.Y., Zhao, K.D., Ling, H.F., 2006. Petrogenesis of Late Jurassic Qianlishan granites and mafic dikes, Southeast China: implications for a back-arc extension setting. Geological Magazine 143, 457–474.
Jiang, Y.H., Zhao, P., Zhou, Q., Liao, S.Y., Jin, G.D., 2011. Petrogenesis and tectonic implications of early cretaceous S- and A-type granites in the northwest of the Gan-Hang rift, SE China. Lithos 121, 55–73.
King, P.L., White, A.J.R., Chappell, B.W., 1997. Characterization and origin of aluminous A-type granites of the Lachlan Fold Belt, Southeastern Australia. Journal of Petrology 36, 371–391.
Klemd, R., Gao, J., Li, J.L., Meyer, M., 2015. Metamorphic evolution of (ultra)-high-pressure subduction-related transient crust in the South Tianshan Orogen (central Asian Orogenic Belt): geodynamic implications. Gondwana Research 28, 1–25.
Kröner, A., Alexeiev, D.V., Rojas-Agramonte, Y., Hegner, E., Wong, J., Xia, X., Belousova, E., Mikolaichuk, A.V., Seltmann, R., Liu, D., 2013. Mesoproterozoic (Grenville-age) terranes in the Kyrgyz north Tianshan: zircon ages and Nd–Hf isotopic constraints on the origin and evolution of basement blocks in the southern Central Asian Orogen. Gondwana Research 23, 272–295.
Lei, R.X., Wu, C.Z., Gu, L.X., Zhang, Z.Z., Chi, G.X., Jiang, Y.H., 2011. Zircon U–Pb chronology and Hf isotope of the Xingxingxia granodiorite from the Central Tianshan zone (NW China): implications for the tectonic evolution of the southern Altaids. Gondwana Research 20, 582–593.
Li, C., Xiao, W.J., Han, C.M., Zhou, K.F., Zhang, J.E., Zhang, Z.X., 2015. Late Devonian–early Permian accretionary orogenesis along the North Tianshan in the southern Central Asian Orogenic Belt. International Geology Review 57, 1023–1050.
Long, L.L., Gao, J., Klemd, R., Beier, C., Qian, Q., Zhang, X., Wang, J.B., Jiang, T., 2011. Geochemical and geochronological studies of granitoid rocks from the Western Tianshan Orogen: implications for continental growth in the southwestern Central Asian Orogenic Belt. Lithos 126, 321–340.
Ma, X.X., Shu, L.S., Meert, J.G., Li, J.Y., 2014. The Paleozoic evolution of Central Tianshan: geochemical and geochronological evidence. Gondwana Research 25, 797–819.
Ma, X.X., Shu, L.S., Meert, J.G., 2015. Early Permian slab breakoff in the Chinese Tianshan belt inferred from the post–collisional granitoids. Gondwana Research 27, 228–243.
Maniar, P.D., Piccoli, P.M., 1989. Tectonic discrimination of granitoids. Geological Society of America Bulletin 101, 635–643.
Middlemost, E.A.K., 1994. Naming materials in the magma igneous rock system. Earth Science Reviews 37, 215–224.
Pearce, J.A., 2008. Geochemical fingerprinting of oceanic basalts with applications to ophiolite classification and the search for Archean oceanic crust. Lithos 100 (1–4), 14–48.
Pearce, J.A., Harris, N.B.W., Tindle, A.G., 1984. Trace element discrimination diagrams for the tectonic interpretation of granitic rocks. Journal of Petrology 25, 956–983.
Petford, N., Gallagher, K., 2001. Partial melting of mafic (amphibolitic) lower crust by periodic influx of basaltic magma. Earth and Planetary Science Letters 193, 483–499.
Qi, L., Hu, J., Grégoire, D.C., 2000. Determination of trace elements in granites by inductively coupled plasma mass spectrometry. Talanta 51, 507–513.
Rapp, R.P., Watson, E.B., 1995. Dehydration melting of metabasalt at 8–32 kbar: implications for continental growth and crust–mantle recycling. Journal of Petrology 36, 891–931.
Rudnick, R.L., Gao, S., 2003. The composition of the continental crust. In: Rudnick, R.L. (Ed.), The Crust. Elsevier-Pergamon, Oxford, pp. 1–64.
Scheltens, M., Zhang, L.F., Xiao, W.J., Zhang, J.J., 2015. Northward subduction-related orogenesis of the southern Altaids: constraints from structural and metamorphic analysis of the HP/UHP accretionary complex in Chinese southwestern Tianshan, NW China. Geoscience Frontiers 6, 191–209.
Şengör, A.M.C., Natal'in, B.A., Burtman, U.S., 1993. Evolution of the Altaid tectonic collage and Paleozoic crustal growth in Eurasia. Nature 364, 209–304.
Shi, Y.R., Liu, D.Y., Zhang, Q., Jian, P., Zhang, F.Q., Miao, L.C., 2007. SHRIMP zircon U–Pb dating of the Gangou granitoids, central Tianshan Mountains, Northwest China and tectonic significances. Chinese Science Bulletin 52, 1507–1516.
Shi, W.X., Liao, Q.A., Hu, Y.Q., Yang, Z.F., 2010. Characteristics of Mesoproterozoic granites and their geological significances from Middle Tianshan Block, East Tianshan District, NW China. Geological Science and Technology Information 29, 29–37 (in Chinese with English abstract).
Sun, S.S., McDonough, W.F., 1989. Chemical and isotopic systematics of oceanic basalts: implications for mantle composition and processes. In: Saunders, A.D., Norry, M.J. (Eds.), Magmatism in the Ocean Basins. Geological Society, London, Special Publications Vol. 42, pp. 313–345.
Sun, L.H., Wang, Y.J., Fan, W.M., Zi, J.W., 2008. Post-collisional potassic magmatism in the Southern Awulale Mountain, western Tianshan Orogen: petrogenetic and tectonic implications. Gondwana Research 14, 383–394.
Tang, G.J., Wang, Q., Wyman, D.A., Sun, M., Li, Z.X., Zhao, Z.H., Sun, W.D., Jia, X.H., Jiang, Z.Q., 2010. Geochronology and geochemistry of Late Paleozoic magmatic rocks in the Lamasu–Dabate area, northwestern Tianshan (West China): evidence for a tectonic transition from arc to post–collisional setting. Lithos 119, 393–411.
Tang, G.J., Wang, Q., Wyman, D.A., Li, Z.X., Xu, Y.G., Zhao, Z.H., 2012. Metasomatized lithosphere–asthenosphere interaction during slab roll–back: evidence from Late Carboniferous gabbros in the Luotuogou area, Central Tianshan. Lithos 155, 67–80.
Tang, G.J., Chung, S.L., Wang, Q., Wyman, D.A., Dan, W., Chen, H.Y., Zhao, Z.H., 2014. Petrogenesis of a Late Carboniferous mafic dike–granitoid association in the western Tianshan: response to the geodynamics of oceanic subduction. Lithos 202–203, 85–99.
Uyeda, S., Kanamori, H., 1979. Back-arc opening and the mode of subduction. Journal of Geophysical Research 84, 1049–1062.
Valley, J.W., Lackey, J.S., Cavosie, A.J., Clechenko, C.C., Spicuzza, M.J., Basei, M.A.S., Bindeman, I.N., Ferreira, V.P., Sial, A.N., King, E.M., Peck, W.H., Sinha, A.K., Wei, C.S., 2005. 4.4 billion years of crustal maturation: oxygen isotope ratios of magmatic zircon. Contributions to Mineralogy and Petrology 150, 561–580.
Wang, Q., Zhao, Z.H., Xu, J.F., Wyman, D.A., Xiong, X.L., Zi, F., Bai, Z.H., 2006. Carboniferous adakite-high-Mg andesite-Nb-enriched basaltic rock suites in the Northern Tianshan area: implications for Phanerozoic crustal growth in the Central Asia Orogenic Belt and Cu–Au mineralization. Acta Petrologica Sinica 22 (1), 11–30 (in Chinese with English abstract).
Wang, B., Shu, L.S., Cluzel, D., Faure, M., Charvet, J., 2007. Geochemical constraints on carboniferous volcanic rocks of the Yili Block (Xinjiang, NWChina): implication for the tectonic evolution of Western Tianshan. Journal of Asian Earth Sciences 29, 148–159.
Wang, B., Faure, M., Shu, L., de Jong, K., Charvet, J., Cluzel, D., Jahn, B.M., Chen, Y., Ruffet, G., 2010. Structural and geochronological study of high-pressure metamorphic rocks in the Kekesu Section (Northwestern China): implications for the late Paleozoic tectonics of the southern Tianshan. Journal of Geochemistry 118, 59–77.
Wang, B., Shu, L., Faure, M., Jahn, B.M., Cluzel, D., Charvet, J., Chung, S.l., Meffre, S., 2011. Paleozoic tectonics of the southern Chinese Tianshan: insights from structural, chronological and geochemical studies of the Heiyingshan ophiolitic melange (NW China). Tectonophysics 497, 85–104.
Whalen, J.B., Currie, K.L., Chappell, B.W., 1987. A-type granites: geochemical characteristics, discrimination and petrogenesis. Contributions to Mineralogy and Petrology 95, 407–419.
Windley, B.F., Alexeiev, D., Xiao, W., Kröner, A., Badarch, G., 2007. Tectonic models for accretion of the Central Asian Orogenic Belt. Journal of the Geological Society, London 164, 31–47.
Wolf, M.B., Wyllie, P.J., 1994. Dehydration-melting of amphibolite at 10 kbar: the effects of temperature and time. Contributions to Mineralogy and Petrology 115, 369–383.
Wyllie, P.J., Wolf, M.B., 1993. Amphibolite dehydration-melting: sorting out the solidus. Geological Society, London, Special Publications 76, 405–416.
Xia, L.Q., Xia, Z.C., Xu, X.Y., Li, X.M., Ma, Z.P., Wang, L.S., 2004a. Carboniferous Tianshan igneous megaprovince and mantle plume. Geological Bulletin of China 23, 903–910 (in Chinese with English abstract).
Xia, L.Q., Xu, X.Y., Xia, Z.C., Li, X.M., Ma, Z.P., Wang, L.S., 2004b. Petrogenesis of carboniferous rift-related volcanic rocks in the Tianshan, Northwestern China. Geological Society of America Bulletin 116, 419–433.
Xia, L.Q., Xia, Z.C., Xu, X.Y., Li, X.M., Ma, Z.P., 2008. Relative contributions of crust and mantle to the generation of the Tianshan Carboniferous rift-related basic lavas, Northwestern China. Journal of Asian Earth Sciences 31, 357–378.
Xiao, W.J., Santosh, M., 2014. The western central Asian Orogenic Belt: a window to accretionary orogenesis and continental growth. Gondwana Research 25, 1429–1444.
Xiao, W.J., Windley, B.F., Badarch, G., Sun, S., Li, J.L., Qin, K.Z., Wang, Z.H., 2004. Palaeozoic accretionary and convergent tectonics of the southern Altaids: implications for the lateral growth of Central Asia. Journal of the Geological Society of London 161, 339–342.
Xiao, W.J., Han, C.M., Yuan, C., Sun, M., Lin, S.F., Chen, H.L., Li, Z.L., Li, J.L., Sun, S., 2008. Middle Cambrian to Permian subduction–related accretionary orogenesis of North Xinjiang, NW China: implications for the tectonic evolution of Central Asia. Journal of Asian Earth Sciences 32, 102–117.
Xiao, W.J., Windley, B.F., Huang, B.C., Han, C.M., Yuan, C., Chen, H.L., Sun, M., Sun, S., Li, J.L., 2009a. End-Permian to mid-Triassic termination of the accretionary processes of the southern Altaids: implications for the geodynamic evolution, Phanerozoic continental growth, and metallogeny of Central Asia. International Journal of Earth Sciences 98, 1189–1287.
Xiao, W.J., Windley, B.F., Yuan, C., Sun, M., Han, C.M., Lin, S.F., Chen, H.L., Yan, Q.R., Liu, D.Y., Qin, K.Z., Li, J.L., Sun, S., 2009b. Paleozoic multiple subduction–accretion processes of the southern Altaids. American Journal of Science 309, 221–270.
Xiao, W.J., Windley, B.F., Allen, M., Han, C.M., 2013. Paleozoic multiple ccretionary and collisional tectonics of the Chinese Tianshan orogenic collage. Gondwana Research 23, 1316–1341.
Xiao, W.J., Han, C.M., Liu, W., Wan, B., Zhang, J.E., Ao, S.J., Zhang, Z.Y., Song, D.F., Tian, Z.H., Luo, J., 2014. How many sutures in the southern Central Asian Orogenic Belt: insights from East Xinjiang–West Gansu (NW China)? Geoscience Frontiers 5, 525–536.
Xiao, W.J., Sun, M., Santosh, M., 2015. Continental reconstruction and metallogeny of the Circum–Junggar areas and termination of the southern Central Asian Orogenic Belt. Geoscience Frontiers 6, 137–140.
Xie, L.W., Zhang, Y.B., Zhang, H.H., Sun, J.F., Wu, F.Y., 2008. In situ simultaneous determination of trace elements, U–Pb and Lu–Hf isotopes in zircon and baddeleyite. Chinese Science Bulletin 53, 1565–1573.
Xu, X.Y., Xia, L.Q., Ma, Z.P., Wang, Y.B., Xia, Z.C., Li, X.M., Wang, L.S., 2006. SHRIMP zircon U–Pb geochronology of the plagiogranites from Bayringou ophiolite in North Tianshan Mountains and the petrogenesis of the ophiolite. Acta Petrologica Sinica 22, 83–94 (in Chinese with English abstract).
Xu, X.Y., Wang, H.L., Li, P., Chen, J.L., Ma, Z.P., Zhu, T., Wang, N., Dong, Y.P., 2013. Geochemistry and geochronology of Paleozoic intrusions in the Nalati (Narati) area in western Tianshan, Xinjiang, China: implications for Paleozoic tectonic evolution. Journal of Asian Earth Sciences 72, 33–62.

Yang, T.N., Li, J.Y., Sun, G.H., Wang, Y.B., 2006. Earlier Devonian active continental arc in central Tianshan: evidence of geochemical analyses and zircon SHRIMP dating on mylonitized granitic rock. Acta Petrologica Sinica 22, 41–48 (in Chinese with English abstract).

Yi, Z.Y., Huang, B.C., Xiao, W.J., Yang, L.K., Qiao, Q.Q., 2015. Paleomagnetic study of Late Paleozoic rocks in the Tacheng Basin of West Junggar (NW China): implications for the tectonic evolution of the western Altaids. Gondwana Research 27, 862–877.

Yin, J.Y., Long, X.P., Yuan, C., Sun, M., Zhao, G.C., Geng, H.Y., 2013. A Late Carboniferous slab window: geochronological and geochemical evidence from mafic to intermediate dykes in West Junggar, NW China. Lithos 175–176, 146–162.

Yin, J.Y., Chen, W., Xiao, W.J., Zhang, B., Cai, K.D., Sun, J.B., Zhang, Y., Yang, J., Yang, L., Liu, X.Y., Shen, Z., 2015a. LA-ICP-MS zircon U–Pb age and geochemistry of the mafic dykes in Central Tianshan Block. Geological Bulletin of China 34 (8), 1469–1480 (in Chinese with English abstract).

Yin, J.Y., Chen, W., Xiao, W.J., Yuan, C., Sun, M., Tang, G.J., Yu, S., Long, X.P., Cai, K.D., Geng, H.Y., Zhang, Y., Liu, X.Y., 2015b. Petrogenesis of Early–Permian sanukitoids from West Junggar, Northwest China: implications for Late Paleozoic crustal growth in Central Asia. Tectonophysics http://dx.doi.org/10.1016/j.tecto.2015.01.005.

Yuan, C., Sun, M., Wilde, S., Xiao, W., Xu, Y., Long, X., Zhao, G., 2010. Post–collisional plutons in the Balikun area, East Chinese Tianshan: evolving magmatism in response to extension and slab break-off. Lithos 119, 269–288.

Zhang, C., Zhai, M.G., Allen, M.B., Sounders, A.D., Wang, G.R., Huang, X., 1993. Implications of Palaeozoic ophiolites from Western Junggar, NW China, for the tectonics of Central Asia. Journal of the Geological Society 150, 551–561.

Zhang, C.L., Li, X.H., Li, Z.X., Ye, H.M., Li, C.N., 2008. A Permian layered intrusive complex in the western Tarim Block, northwestern China: product of a ca.275 Ma mantle plume? Journal of Geology 116, 112–128.

Zhang, C.L., Xu, Y.G., Li, Z.X., Wang, H.Y., 2010. Diverse Permian magmatism in the Tarim Block, NW China: genetically linked to the Permian Tarim mantle plume? Lithos 119, 537–552.

Zhang, Y.Y., Yuan, C., Sun, M., Long, X.P., Xia, X.P., Wang, X.Y., Huang, Z.Y., 2015. Permian doleritic dikes in the Beishan Orogenic Belt, NW China: asthenosphere–lithosphere interaction in response to slab break-off. Lithos 233, 174–192.

Zhao, Z.Y., Zhang, Z.C., Santosh, M., Huang, H., Cheng, Z.G., Ye, J.C., 2015. Early Paleozoic magmatic record from the northern margin of the Tarim Craton: further insights on the evolution of the Central Asian Orogenic Belt. Gondwana Research 28, 328–347.

Zhou, M.F., Arndt, N.T., Malpas, J., Wang, C.Y., Kennedy, A.K., 2008. Two magma series and associated ore deposits types in the Permian Emeishan large igneous province, SW China. Lithos 103, 352–368.

Zhu, B.Q., Wang, L.S., Wang, L.X., 1987. Paleozoic era ophiolite of southwest part in western Junggar, Xinjiang, China. Bulletin of the Xi'an Institute of Geology and Mineral Resources, The Chinese Academy of Geological Sciences 17, 3–64 (in Chinese with English abstract).

Zhu, Y.F., Zhang, L.F., Gu, L.B., Guo, X., Zhou, J., 2005. Study on trace elements geochemistry and SHRIMP chronology of Carboniferous lava, West Tianshan. Chinese Science Bulletin 50, 2201–2212.

Zhu, Y.F., Guo, X., Song, B., Zhang, L.F., Gu, L.B., 2009. Petrology, Sr–Nd–Hf isotopic geochemistry and zircon chronology of the Late Palaeozoic volcanic rocks in the southwestern Tianshan Mountains, Xinjiang, NW China. Journal of the Geological Society of London 166, 1085–1099.

Zhu, W., Charvet, J., Xiao, W., Jahn, B.M., 2011. Continental accretion and intracontinental deformation of the Central Asian Orogenic Belt. Journal of Asian Earth Sciences 42, 769–773.